IoT-5G user tracking in a 5G network using 60 GHz mm-waves based on an ABF-ED algorithms for a cluttered indoor environment

H. E. ADARDOUR [1,3] *, S. KAMECHE [2,3], S.M.H. IRID [2,3], O. BENMOSTEFA [2], A. A. BENAMAR [2]

[1] Department of Electronics, Faculty of Technology, University Hassiba Benbouali, Chlef, Algeria - h.adardour@univ-chlef.dz
[2]Department of Telecommunications, Faculty of Technology, University Abou Bekr Belkaid, Tlemcen, Algeria –(samir.kameche, sidimohammedhadj.irid)@univ-tlemcen.dz, (benmostefaothmane, messim944)@gmail.com
[3] STIC Laboratory, Faculty of Technology, University Abou Bekr Belkaid, Tlemcen, Algeria

KEY WORDS: IoT, 5G, 60 GHz, Mm-waves, Channel propagation, Path loss, ABF-ED.

ABSTRACT:

This paper presents a user tracking algorithm in an IoT-5G Network (or IoT-5GN). Hereby, we aim at studying and evaluating the sensing performances of the IoT-5G Access Point (or IoT-5G AP) primary signal by the IoT-5G user in a cluttered indoor environment using an energy detector (or ED) algorithm and an Alpha-&-Beta Filter (ABF or α-β-F) estimator. The 5G primary signal (or 5G-PS) frequency that we would like to detect is: 60 GHz. As a result, the 5G-PS sensing via the proposed ABF-ED algorithm, enabled us to track the IoT-5G user inside of the IoT-5G AP coverage area. The performances of the proposed ABF-ED algorithm in this paper work is evaluated by the probability of total detection error (or PTDE) measure. Through different scenarios simulations, the performances and robustness of the proffered algorithm are demonstrated.

1. INTRODUCTION

In the current day and age, with the advancement of IoT (or Internet of Things) application technology era, the growth is becoming increasingly dense (Mohanty et al., 2021). As a result, the Wireless-Local Area Network (or W-LAN) technology which leverages the millimeter Waves (or mmWs) around the 60 GHz frequency has been selected due to its flexibility, low cost and other advantages compared to the Wired Network (or WN), and this making its suitable for IoT applications. As such, there is considerable demand for high-throughput Wireless Communications (or WCs) (Saha et al., 2021).

The huge demand for bandwidth and higher data rates has resulted in many spectrum bands growing more congested and the ability to provide a more efficient network is increasingly required. Simultaneously, there is a large amount of unlicensed spectrum in the 60 GHz range (or in mmWs) which is not being leveraged (Sahoo et al., 2021). Currently, the WCs systems have became a critical part of one's day-to-day life and are constantly evolving to offer a better quality and experience to the users (Azzahra et al., 2021; Yong et al., 2011; Nitsche et al., 2014).

Nevertheless, mmWs technology is one of the most prominent emerging WCs technologies in recent years. (Herschfelt et al., 2021). Although this technology has been available for decades, the advances in silicon process technology and low-cost integration solutions have enabled this technology (i.e., mmWs) to become commercially applicable only within the last seven to eight years (Azzahra et al., 2021; Yong et al., 2011; Nitsche et al., 2014).

Drawing on the afore-stated idea, the mmWs technology has attracted considerable interest from academia, industry and standards agencies. The 60 GHz IoT technology offers various advantages compared to current or existing WCs systems. The availability of a large spectrum band around 60 GHz for unlicensed employment on a global scale is resulting in the emergence of new technologies enabling the Wi-Fi communication under this frequency band. However, the propagation of signals at 60 GHz differs considerably compared to the 2.4 and 5 GHz bands (Azzahra et al., 2021; Yong et al., 2011; Nitsche et al., 2014).

For this reason, the objective of this research is to study and evaluate the sensing performances of a 5G primary signal (or 5G-PS) at 60 GHz, in order to track a IoT-5G user in an IoT-5G Network (or IoT-5GN) for the upcoming generation IoT applications based on a proposed algorithm called the 5G Signal Sensing Cycle (or SSC) using the Alpha-&-Beta Filter (or α-β-F) estimator and the energy detector (or ED) algorithm (Adardour and Kameche, 2019; Adardour et al., 2015).

For the sake of achieving the stated objective, this research consists of three sections that follow a general introduction of the 60 GHz technology. In Section 2, we discuss the proposed 5G-PS sensing algorithm. The simulation and the obtained results are displayed and discussed in Section 3. Finally, we proffer some closing adherences in Section 4.

2. PROPOSED 5G SIGNAL SENSING ALGORITHM

The algorithm we endeavor to study in this paper is composed of two phases; the first one employs an estimator called Alpha-&-Beta Filter (or α-β-F), the second one consists to apply an energy detector (or ED) algorithm (Adardour and Kameche, 2019; Adardour et al., 2015).

Nevertheless, the α-β-F performance, which is exploited in the present work, will be summed up in below sub-sections. It is worth recalling that the α-β-F is a simplified version of the Kalman Filter Estimator (or KF-E), which can reliably estimate and track the position of a mobile node (in this case, an IoT-5G user), that may be located anywhere, with a minimum estimation error. The α-β-F has also numerous applications in a wide range of fields. The primary advantage of this filter is that the system process noise is not considered. Instead, the system process noise is accounted for the KF-E, which is a drawback for us (Adardour and Kameche, 2019).

* Corresponding author

Besides all the different PS detection strategies in the literature. We also employed the ED (or radiometer), the ED has been regarded as a promising key factor due to its easy implementation, it requires no previous information on the detected signal, and its low cost of computing and efficiency for a high SNR (or Signal-per-Noise Ratio) (Adardour et al., 2015).

As previously mentioned in the introduction, the aim of this work is to study and evaluate the performance of real-time detection of a 5G-PS (or IoT-5G Access Point (IoT-5G AP)) with the impact mobility of a IoT-5G user (consult Fig. 1); out contribution is based on the following:

Phase one (α-β-F):

- The first stage is to estimate the position and speed of an IoT-5G user.
- The second stage is focused on the estimation of the received signal power (or RSP) at the IoT-5G user under two propagation models (Log-Distance Path Loss (or LD-PL) and Log-Normal Shadowing Path Loss (or LNS-PL)).
- The last stage is devoted to estimate the SNR at all links amid the IoT-5G AP and the IoT-5G user.

Phase two (ED):

By means of the SNR estimation, the presence or absence of the 5G-PS coming from the IoT-5G AP at 60 GHz frequency can be predicted.

As illustrated in Fig. 1, we consider the proposed IoT-5GN in this study composed of:

- IoT-5G AP situated in an IoT-5GN with the following coordinate: (0,0).
- The IoT-5G user is semi-randomly deployed in an IoT-5GN with the following coordinate: $\left(x_{i(IoT-5G\ user)}, y_{j(IoT-5G\ user)}\right)$.

Subsequently, we present the 5G SSC algorithm that will be carried out throughout this work with the three sub-sections; which are modeled by mathematical equations.

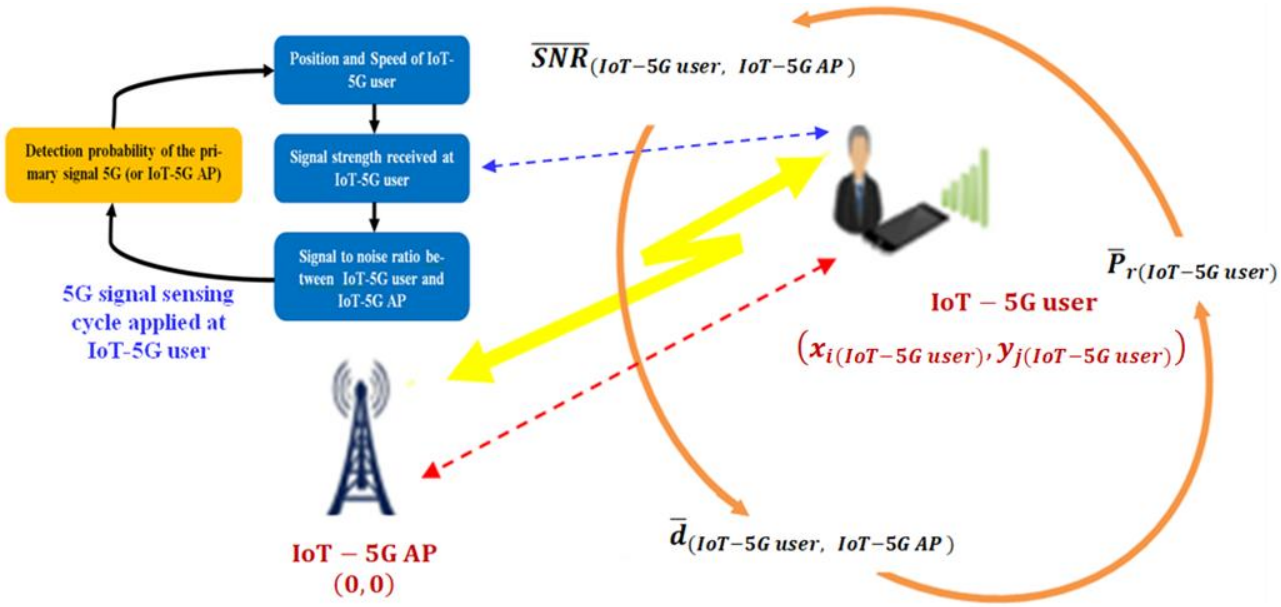

Figure 1. 5G signal sensing cycle (or 5G SSC) and IoT-5G network.

2.1 IoT-5G user tracking via α-β-F

Here, the position and speed of an IoT-5G user node were estimated using the α-β-F based on a constant acceleration model of the target (or IoT-5G user), and this was performed via the application of both filter gains, namely the alpha (α) and beta (β) filters. The α-β-F is a two-stage filter; both stages representing the prediction process and the smoothing process (Adardour and Kameche, 2019):

Stage 1: The prediction process may be formulated as follows (Adardour and Kameche, 2019):

On the X − axis :

$$\begin{cases} x_{p(i)} = x_{s(i-1)} + T \cdot v_{xs(i-1)} + \left(\frac{T^2}{2}\right) \cdot acc_{xs(i-1)} \\ v_{xp(i)} = v_{xs(i-1)} + T \cdot acc_{xs(i-1)} \end{cases} \quad (1)$$

On the Y − axis :

$$\begin{cases} y_{p(j)} = y_{s(j-1)} + T \cdot v_{ys(j-1)} + \left(\frac{T^2}{2}\right) \cdot acc_{ys(j-1)} \\ v_{yp(j)} = v_{ys(j-1)} + T \cdot acc_{ys(j-1)} \end{cases} \quad (2)$$

Where T denotes the sampling interval or the time step, $\left(x_{(i)}, y_{(j)}\right)$ is the position, $\left(v_{x(i)}, v_{y(j)}\right)$ is the speed, $\left(acc_{x(i)}, acc_{y(j)}\right)$ is the acceleration; p and s relate to the predicted and smoothed state variables respectively.

The Eqs. (1) and (2) can be otherwise written as follows (Adardour and Kameche, 2019):

$$\begin{aligned} x_{p(i)} &= x_{s(i-1)} + T \cdot v_{xs(i-1)} + \left(\frac{T^2}{2}\right) \cdot acc_{xs(i-1)} \\ \langle y_{p(j)} &= y_{s(j-1)} + T \cdot v_{ys(j-1)} + \left(\frac{T^2}{2}\right) \cdot acc_{ys(j-1)} \rangle \\ v_{xp(i)} &= v_{xs(i-1)} + T \cdot acc_{xs(i-1)} \\ v_{yp(j)} &= v_{ys(j-1)} + T \cdot acc_{ys(j-1)} \end{aligned} \quad (3)$$

The development of the system can be expressed as a matrix according to Eq. (3) as follows (Adardour and Kameche, 2019):

$$\begin{aligned} X_{p(k)} &= \langle {x_{p(i)} \atop y_{p(j)}} \rangle \\ X_{p(k)} &= \begin{bmatrix} 1 & 0 \\ 0 & 1 \end{bmatrix} \cdot \begin{bmatrix} x_{s(i-1)} \\ y_{s(j-1)} \end{bmatrix} + \begin{bmatrix} T & 0 \\ 0 & T \end{bmatrix} \cdot \begin{bmatrix} v_{xs(i-1)} \\ v_{ys(j-1)} \end{bmatrix} + \cdots \\ &\quad \cdots + \begin{bmatrix} T^2/2 & 0 \\ 0 & T^2/2 \end{bmatrix} \cdot \begin{bmatrix} acc_{xs(i-1)} \\ acc_{ys(j-1)} \end{bmatrix} \\ X_{p(k)} &= \Phi \cdot X_{s(k-1)} + H \cdot V_{s(k-1)} + \Gamma \cdot acc_{s(k-1)} \end{aligned} \quad (4)$$

And

$$\begin{aligned} V_{p(k)} &= \langle {v_{xp(i)} \atop v_{yp(j)}} \rangle \\ V_{p(k)} &= \begin{bmatrix} 1 & 0 \\ 0 & 1 \end{bmatrix} \cdot \begin{bmatrix} v_{xs(i-1)} \\ v_{ys(j-1)} \end{bmatrix} + \begin{bmatrix} T & 0 \\ 0 & T \end{bmatrix} \cdot \begin{bmatrix} acc_{xs(i-1)} \\ acc_{ys(j-1)} \end{bmatrix} \\ V_{p(k)} &= \Lambda \cdot V_{s(k-1)} + \Psi \cdot acc_{s(k-1)} \end{aligned} \quad (5)$$

Stage 2: In the light of the previously predicted values, which were established in the first stage, the smoothing process can be expressed by the following formulas (Adardour and Kameche, 2019):

$$X_{s(k)} = X_{p(k)} + \alpha \cdot (X_{0(k)} - X_{p(k)}) \quad (6)$$

$$V_{s(k)} = V_{p(k)} + \left(\frac{\beta}{T}\right) \cdot (X_{0(k)} - X_{p(k)}) \quad (7)$$

Where, $X_{0(k)}$ is the actual position node of IoT-5G user.

Once the α-β-F has been applied to estimate the position and speed of IoT-5G user, the link distance between the IoT-5G AP and the IoT-5G user can be estimated, which will be integrated into the propagation models required to estimate the RSP at the IoT-5G user (or $\bar{P}_{r(IoT-5G\ user)}$) and the SNR of each link between the IoT-5G AP and the IoT-5G user.

2.2 5G signal propagation model

The estimate of the RSP in dB coming from the IoT-5G AP to the IoT-5G user is expressed as:

$$\begin{aligned} \bar{P}_{r(IoT-5G\ user)} &= P_{r(IoT-5G\ user)}(d_0) - \cdots \\ &\quad \cdots - \left(10 \cdot E_{PL(LOS/NLOS)} log_{10}\left(D_{\bar{d}/d_0}\right)\right) \end{aligned} \quad (8)$$

Where,

$$P_{r(IoT-5G\ user)}(d_0) = P_{t(IoT-5G\ AP)} - PL_0 \quad (9)$$

$$PL_0 = 20log_{10}\left(\frac{4\pi d_0}{\lambda}\right) \quad (10)$$

$$D_{\bar{d}/d_0} = \frac{\bar{d}_{(IoT-5G\ user,IoT-5G\ AP)}}{d_0} \quad (11)$$

It is assumed from Eq. (8) that the LD-PL model is expressed as:

$$\left[\frac{\bar{P}_{r(IoT-5G\ user)}\left(\bar{d}_{(IoT-5G\ user,IoT-5G\ AP)}\right)}{P_{r(IoT-5G\ user)}(d_0)}\right]_{[dB]} = -10 \cdot E_{PL(LOS/NLOS)} \cdot log_{10}\left(D_{\bar{d}/d_0}\right) \quad (12)$$

Furthermore, to obtain the model of LNS-PL, we append an additional factor $X_{\sigma(LOS/NLOS)}$ in the LD-PL model, and this corresponding model:

$$\left[\frac{\bar{P}_{r(IoT-5G\ user)}\left(\bar{d}_{(IoT-5G\ user,IoT-5G\ AP)}\right)}{P_{r(IoT-5Guser)}(d_0)}\right]_{[dB]} = -10 \cdot E_{PL(LOS/NLOS)} \cdot log_{10}\left(D_{\bar{d}/d_0}\right) + X_{\sigma(LOS/NLOS)} \quad (13)$$

Where, $\bar{P}_{r(IoT-5G\ user)}$, $P_{t(IoT-5G\ AP)}$, PL_0, $\bar{d}_{(IoT-5G\ user,IoT-5G\ AP)}$, λ and $E_{PL(LOS/NLOS)}$, are accordingly, the RSP estimation at the IoT-5G user in [dB], the PS coming from the IoT-5G AP in [dB], the PL at the reference distance d_0 in [dB], the estimated link distance amid the IoT-5G user and the IoT-5G AP in [m], the wavelength of the 5G-PS in [mm], and the exponent of PL in LOS (i.e. line-of-sight) or in NLOS (i.e. none of line-of-sight). In addition, $X_{\sigma_{(LOS/NLOS)}}$ is a GRV (or Gaussian Random Variable) distributed with zero mean and standard deviation $\sigma_{(LOS/NLOS)}$ in [dB].

However, to compute the link of the $\overline{SNR}_{(IoT-5G\ user,IoT-5G\ AP)}$ of the estimated distance $\bar{d}_{(IoT-5G\ user,IoT-5G\ AP)}$amid the IoT-5G user and the IoT-5G AP, we rely on the following equation:

$$\overline{SNR}_{(IoT-5G\ user,IoT-5G\ AP)} = \frac{\bar{P}_{r(IoT-5G\ user)}}{P_{Noise}} \quad (14)$$

$$\overline{SNR}_{(IoT-5G\ user,IoT-5G\ AP)_{[dB]}} = 10 \cdot log_{10}\left(\frac{\bar{P}_{r(IoT-5G\ user)}}{P_{Noise}}\right) \quad (15)$$

$$\begin{aligned} \overline{SNR}_{(IoT-5G\ user,IoT-5G\ AP)_{[dB]}} &= \bar{P}_{r(IoT-5G\ user)_{[dB]}} - \cdots \\ &\quad \cdots - P_{Noise_{[dB]}} \end{aligned} \quad (16)$$

Namely, P_{Noise} refers to the noise power of the used IoT-5GN environment (where, the IoT-5G AP has been installed) (Adardour and Kameche, 2019).

2.3 Local 5G signal sensing model

In this sub-section, we will present the local 5G-PS sensing model. Nevertheless, the process of 5G spectrum sensing or IoT-5G AP (i.e. 5G-PS) sensing is divided into two phases: Local 5G-PS sensing (or L-5G-PSS) and Cooperative 5G-PS sensing (or C-5G-PSS). In this contribution, we apply on the L-5G-PSS technique. For L-5G-PSS, we consider that the IoT-5G user is embedded with an ED to detect the 5G-PS in order to identify whether the IoT-5G AP is present or absent in the area of interest (refer to the Fig. 1). It may be formulated as follows (Adardour et al., 2015):

In the absence of IoT-5G AP, the estimate of the RSP at the IoT-5G user is expressed as:

$$S_{\bar{P}_{r(IoT-5G\ user)}}(t) = w(t) \leftrightarrows H_0 \quad (17)$$

In the presence of IoT-5G AP, the estimate of the RSP at the IoT-5G user is expressed as:

$$S_{\bar{P}_{r(IoT-5G\ user)}}(t) = S_{P_{t(IoT-5G\ AP)}}(t) + w(t) \leftrightarrows H_1 \quad (18)$$

Where, $S_{\bar{P}_{r(IoT-5G\ user)}}(t)$ is the estimated value of the RSP towards the IoT-5G user, $S_{P_{t(IoT-5G\ AP)}}(t)$ is the 5G-PS coming from the IoT-5G AP and $w(t)$ denotes the Additive White Gaussian Noise (or AWGN). Through the observation of $S_{\bar{P}_{r(IoT-5G\ user)}}(t)$, the IoT-5G user has to decide amid H_0 (i.e. IoT-5G AP is missing) and H_1(i.e. IoT-5G AP is active).

If we assume that $E_{S_{\bar{P}_{r(IoT-5G\ user)}}}$ is the energy of $S_{\bar{P}_{r(IoT-5G\ user)}}(t)$, it may be stated as:

$$E_{S_{\bar{P}_{r(IoT-5G\ user)}}} = \left(\frac{1}{M}\right)\sum_{n=1}^{M}\left|S_{\bar{P}_{r(IoT-5G\ user)}n}\right|^2 \quad (19)$$

Where, $S_{\bar{P}_{r(IoT-5G\ user)}n}$ is a sample obtained from the estimated value of the RSP towards the IoT-5G user and $M = 2 \cdot T \cdot W$ is the number of total samples. So, the estimated value of the RSP towards the IoT-5G user will be detected under an bandwidth W pending an observation period T.

Furthermore, the output energy ($E_{S_{\bar{P}_{r(IoT-5G\ user)}}}$) of ED is distributed as follows:

$$\begin{cases} E_{S_{\bar{P}_{r(IoT-5G\ user)/H_0}}} = \left(\frac{1}{M}\right)\sum_{n=1}^{M}|w_n|^2 \\ E_{S_{\bar{P}_{r(IoT-5G\ user)/H_1}}} = \left(\frac{1}{M}\right)\sum_{n=1}^{M}\left|S_{P_{t(IoT-5G\ AP)}n} + w_n\right|^2 \end{cases} \quad (20)$$

The equation (20) can be written as follows:

$$\begin{cases} E_{S_{\bar{P}_{r(IoT-5G\ user)/H_0}}} = \chi_M^2 \\ E_{S_{\bar{P}_{r(IoT-5G\ user)/H_1}}} = \chi_M^2(2\gamma) \end{cases} \quad (21)$$

Where $\gamma = \overline{SNR}_{(IoT-5G\ user,IoT-5G\ AP)_{[dB]}}$, χ_M^2 and $\chi_M^2(2\gamma)$ are the Central Chi-Square Distribution (or CC-SD) and Non-Central Chi-Square Distribution (or NCC-SD) functions, respectively. M is the DF (i.e. Degree of Freedom) (Adardour et al., 2015).

The 5G-PS sensing performances under an AWGN channel are estimated through two parameters: PD (i.e. Probability of Detection) and PFA (i.e. Probability of False Alarm), which are represented as (Adardour et al., 2015):

$$PD = Pr\left(E_{S_{\bar{P}_{r(IoT-5G\ user)}}} > E_T|H_1\right) = Q_M\left(\sqrt{2\overline{SNR}_{(IoT-5G\ user,IoT-5G\ AP)}}, \sqrt{E_T}\right) \quad (22)$$

$$PFA = Pr\left(E_{S_{\bar{P}_{r(IoT-5G\ user)}}} > E_T|H_0\right) = \frac{\Gamma\left(M, \frac{E_T}{2}\right)}{\Gamma(M)} \quad (23)$$

Where $\Gamma(\cdot)$ and $\Gamma(\cdot,\cdot)$ are complete and incomplete gamma functions, respectively. $Q_M(\cdot,\cdot)$ is the generalized Marcum Q-function and E_T is the threshold energy (Adardour et al., 2015).

3. SIMULATION AND RESULTS

In this section, the simulations and results were done with the help of MATLAB 2017a software. What we are interested in scrutinizing in this work, is the anticipation of real-time 5G-PS sensing from the IoT-5G AP with the impact mobility of the IoT-5G user under three scenarios proposed, as shown in Table 1. The parameters of our simulation are enumerated in Table 2 (Sun et al., 2016; Joongheon et al., 2017; Zhang and Yu, 2019).

In this work, the first phase of the proposed algorithm aims at estimating the RSP at the IoT-5G user and the SNR link amid the IoT-5G AP and the IoT-5G user. To do that, we first need to estimate the trajectory (i.e. the position and speed) of the IoT-5G user compared to a reference point, which will be the IoT-5G AP, through the use of α-β-F.

According to Fig. 2, the IoT-5G AP was installed in a closed environment of 130 x 130 [m^2], as shown by the maroon contour, in addition, the two gray squares are considered as obstacles facing the IoT-5G user. However, the Fig. 2 illustrates the real (i.e. red) and estimated (i.e. light blue) trajectory of IoT-5G user in an IoT-5GN. It is clear that the IoT-5G user takes a semi-random trajectory. Consequently, the obtained results led us to conclude that the α-β-F offered high performance in order to track the real trajectory of the IoT-5G user with a lower estimation error for each position of the IoT-5G user (refer to Fig. 3). For example, the estimated average error of the IoT-5G user position is equal to $1.1762 \cdot 10^{-04}$[m].

	5G signal propagation model	Observation channel
Scenario (A)	LD-PL	AWGN
Scenario (B)	LNS-PL ($E_{PL(LOS)}$)	AWGN
Scenario (C)	LNS-PL ($E_{PL(NLOS)}$)	AWGN

Table 1. Local 5G-PS sensing scenarios.

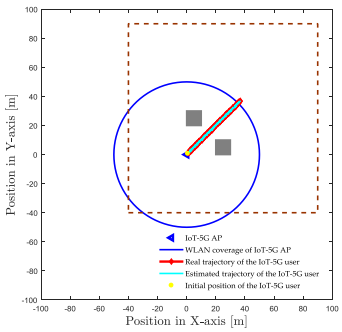

Figure 2. Real and estimated semi-random positions of the IoT-5G user.

Parameters	Values
Coverage area of the IoT-5G AP	50 x 50 [m^2]
Frequency	60 [GHz]
Transmission power of the IoT-5G AP	15 [dBm]
Noise power at the IoT-5G user	−139 [dBm]
Exponent of path loss	$E_{PL(LOS)} = 2.17$ and $E_{PL(NLOS)} = 3.01$
Reference distance	1.0 [m]

Table 2. Simulation parameters.

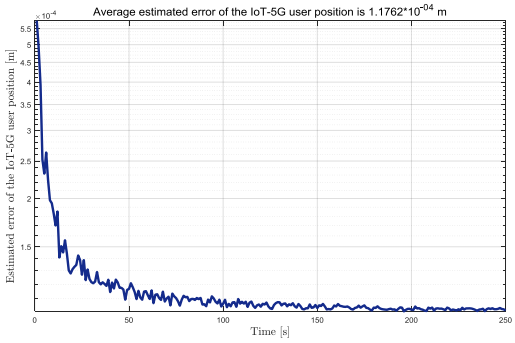

Figure 3. Estimated error of the IoT-5G user position [m] vs. Time [s].

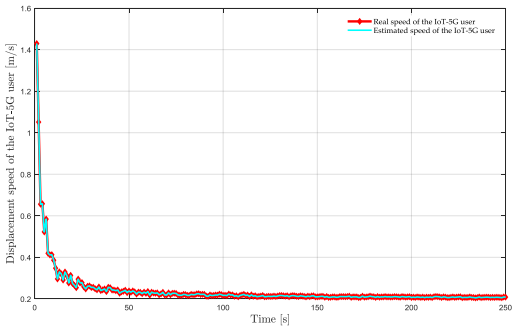

Figure 4. Real and estimated speeds of the IoT-5G user vs. Time [s].

Figure 4 displays the real and estimated speeds for the movement of IoT-5G user in an IoT-5GN. From the obtained results in Fig. 4, one can clearly observe that the estimated speed of IoT-5G user using the α-β-F is similar to the case of the real speed, and consequently a lower estimation error is registered for each speed of the IoT-5G user at each time (refer to Fig. 5). For example, the estimated average error of the IoT-5G user speed is equal to $9.4092 \cdot 10^{-06}$[m/s].

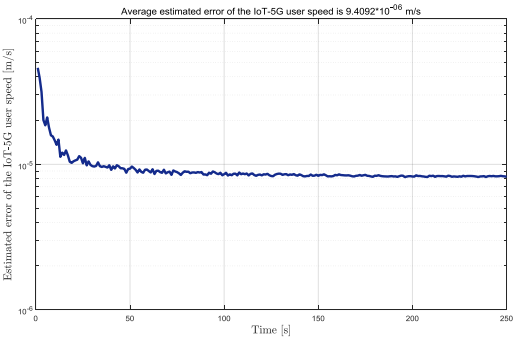

Figure 5. Estimated error of the IoT-5G user speed [m/s] vs. Time [s].

From Eqs. (8) up to (13), we are able to evaluate the real and estimated RSP at the IoT-5G user, as illustrated in Fig. 6. As the IoT-5G user moves further away from the IoT-5G AP (see Fig. 2), the RSP at the IoT-5G user decreases and vice versa (see Fig. 6). In addition, Fig. 6 illustrates the possible variations in the RSP for each the IoT-5G user position, in three propagation models, namely: LD-PL, LNS-PL ($E_{PL(LOS)}$) and LNS-PL ($E_{PL(NLOS)}$). As results, one can clearly notice that the LNS-PL ($E_{PL(NLOS)}$) model can affect the real and estimated RSP at the IoT-5G user (see black color and yellow color, respectively). As a conclusion, the estimation phase of the RSP at the IoT-5G user using the α-β-F, allowed us to identify the 5G-PS coming from the IoT-5G AP with some accuracy, due to the similarity amid the real and estimated results. For example, the estimated average error of the RSP at the IoT-5G user under a LNS-PL ($E_{PL(NLOS)}$) model is $1.5949 \cdot 10^{-04}$ [dBm] (see Fig. 6) and when comparing the estimated error of the RSP at the IoT-5G user for the three proposed scenarios, one can observe that the estimated error under a LNS-PL ($E_{PL(NLOS)}$) model is the most critical compared to the other two propagation models (see Fig. 7).

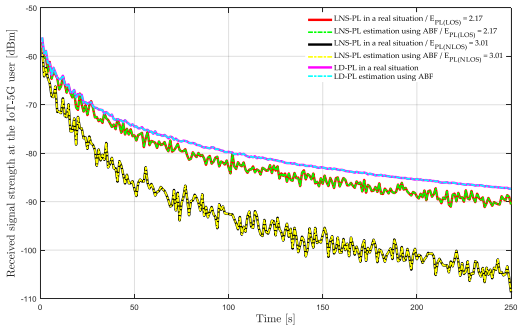

Figure 6. RSP at the IoT-5G user [dBm] vs. Time [s].

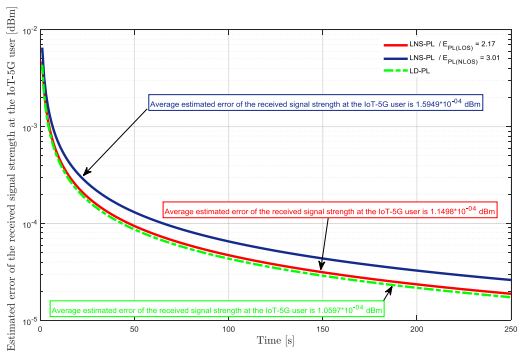

Figure 7. Estimated error of the RSP at the IoT-5G user [dBm] vs. Time [s].

The third scenario (see Table 1) is the most realistic in an IoT-5GN, therefore, the algorithm which we proposed in this paper aims at estimating the sensing level of the 5G-PS from the IoT-5G AP at 60 GHz under an AWGN channel. To do that, we rely on the estimation of the SNR link amid the IoT-5G user and the IoT-5G AP, as shown in Fig. 8. As expected, when the RSP at the IoT-5G user is weakened (see Fig. 6), the SNR link amid the IoT-5G user and IoT-5G AP is also weakened (see Fig. 8), and reciprocally. Regarding the results obtained from the estimated error of the SNR link amid the IoT-5G user and the IoT-5G AP, they take the same rate of the obtained results from the estimated error of the RSP at the IoT-5G user (see Fig. 7 and Fig. 9), because the P_{Noise} at the IoT-5G user has been considered as a constant in this work (see Table 2) and therefore the SNR link amid the IoT-5G user and the IoT-5G AP will be directly correlated to the variation of RSP at the IoT-5G user (consult Eqs. (14), (15) and (16)).

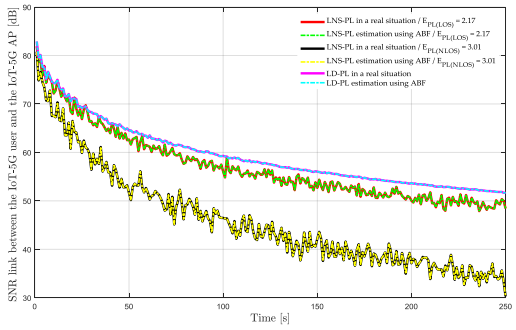

Figure 8. SNR link amid the IoT-5G user and the IoT-5G AP [dB] vs. Time [s].

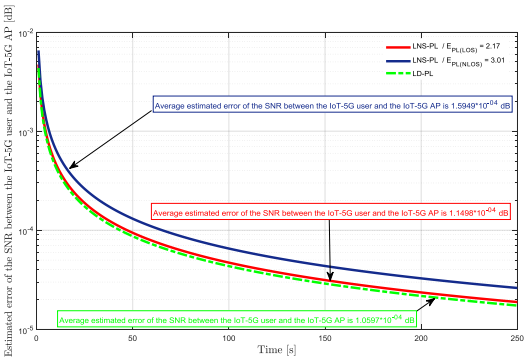

Figure 9. Estimated error of the SNR link amid the IoT-5G user and the IoT-5G AP [dB] vs. Time [s].

Specifically, the second phase of the proposed algorithm aims to estimate the probability of total detection error (or PTDE) of a 5G-PS at 60 GHz from the IoT-5G AP. In Fig. 10, the PTDE as a function of time is displayed for each position of the IoT-5G user in three scenarios as shown in Table 1. For the results that were obtained, the PFA was chosen at 10^{-06}.

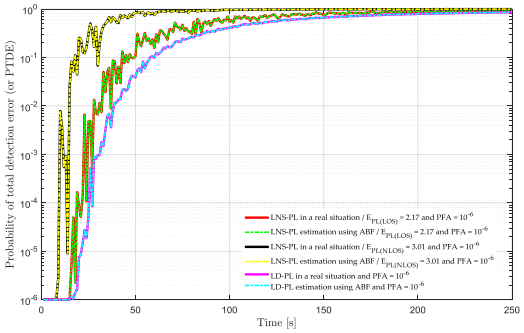

Figure 10. Probability of total detection error vs. Time [s].

It is registered that the obtained results previously in the first phase have a clear influence on the 5G-PS sensing at 60 GHz of the IoT-5G AP. For example, there are some comparative results summarized in Table 3. Indeed, one can clearly notice in Table 3 that there is a very low error in the estimation of the PTDE amid the real case and the estimated case, and even the results obtained in Fig. 11 also proved that the estimated error of the PTDE of a 5G-PS at 60 GHz from the IoT-5G AP is very low. For example, the estimated average errors of the PTDE, are as follows: $1.8681 \cdot 10^{-06}$ (scenario (A)), $2.0785 \cdot 10^{-06}$ (scenario (B)) and $2.4594 \cdot 10^{-06}$ (scenario (C)). However, the PTDE is determined by the following Eq. (24):

$$PTED = 1 - PD + PFA \tag{24}$$

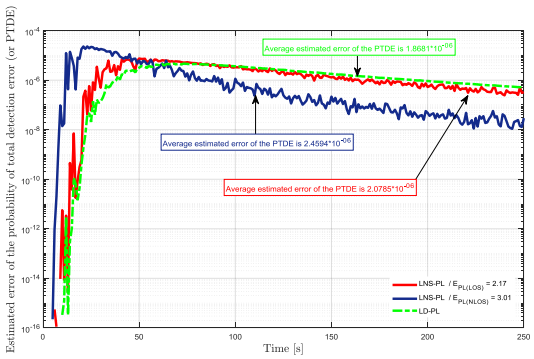

Figure 11. Estimated error of the PTDE vs. Time [s].

t = 100 s	$\mathbf{SNR}_{(IoT-5G\ user, IoT-5G\ AP)}$	$\overline{\mathbf{SNR}}_{(IoT-5G\ user, IoT-5G\ AP)}$	PTDE	$\overline{\mathbf{PTDE}}$
Scenarios (A)	59.2869 dB	59.2868 dB	$10^{-0.3764}$	$10^{-0.3763}$
Scenarios (B)	56.0584 dB	56.0583 dB	$10^{-0.263932}$	$10^{-0.263929}$
Scenarios (C)	46.4833 dB	46.4832 dB	$10^{-0.011826}$	$10^{-0.0118258}$

Table 3. PTDE vs. SNR at 100 s.

4. CONCLUSION

In a nutshell, this paper endeavored to study the performance evaluation of an algorithm that serves in detecting a 5G-PS at 60 GHz coming from the IoT-5G AP in real-time, inside an IoT-5GN. However, we found that the mobility of the IoT-5G user has an adverse effect on the sensing performances of a 5G-PS at 60 GHz in an IoT-5GN, which allows us to verify this influence is: the behavior of the PTDE as a function of the link distance amid the IoT-5G user and the IoT-5G AP. As a result, the algorithm that we proposed uses an estimator which provides excellent results with a minimum estimation error; it is the α-β-F. As a final note, the performances of the proffered algorithm for the IoT-5G user tracking in an IoT-5GN gives attractive results for future IoT applications.

REFERENCES

Adardour, H.E., Kameche, S. 2019. Enhancing the Performance of Spectrum Mobility in Cognitive Radio Local Area Networks Using KF-ABF-SRE Estimators, in Wireless Pers Commun, 104, 1321–1341, https://doi.org/10.1007/s11277-018-6085-7

Adardour, H.E., Meliani, M.,andHachemi, M.H., 2015. Estimation of the Spectrum Sensing for the Cognitive Radios: Test Analysing Using Kalman Filter, in Wireless Pers Commun, 84, 1535–1549. https://doi.org/10.1007/s11277-015-2701-y

Azzahra, M. A., and Iskandar, 2018. Performance of 60 GHz Millimeter-Wave Propagation in Indoor Environment, in: 2018 International Symposium on Electronics and Smart Devices (ISESD), 2018, pp. 1-4, doi: 10.1109/ISESD.2018.8605447

Herschfelt, A., Chiriyath, A. R., Srinivas, S., and Bliss, D. W., 2021. An Introduction to Spectral Convergence: Challenges and Paths to Solutions, in: 2021 1st IEEE International Online Symposium on Joint Communications & Sensing (JC&S), 2021, pp. 1-6, doi: 10.1109/JCS52304.2021.9376388

Joongheon, K., Jae-Jin, L., and Woojoo, L., 2017. Strategic Control of 60 GHz MillimeterWave High-Speed Wireless Links for Distributed Virtual Reality Platforms, in Hindawi, Mobile Information Systems, Volume 2017, Article ID 5040347, 10 pages. https://doi.org/10.1155/2017/5040347

Mohanty, S., Agarwal, A., Agarwal, K., Mali, S., and Misra, G., 2021. Role of Millimeter Wave for Future 5G Mobile Networks: Its Potential, Prospects and Challenges, in: 2021 1st Odisha International Conference on Electrical Power Engineering, Communication and Computing Technology (ODICON), 2021, pp. 1-4, doi: 10.1109/ODICON50556.2021.9429017

Nitsche, T., Cordeiro, C., Flores, A. B., Knightly, E. W., Perahia, E., and Widmer, J. C., 2014. IEEE 802.11ad: directional 60 GHz communication for multi-Gigabit-per-second Wi-Fi [Invited Paper], in IEEE Communications Magazine, 52(12), 132-141, December 2014, doi: 10.1109/MCOM.2014.6979964

Saha, S. K. et al., 2021. Performance and Pitfalls of 60 GHz WLANs Based on Consumer-Grade Hardware, in IEEE Transactions on Mobile Computing, 20(4), 1543-1557, 1 April 2021, doi: 10.1109/TMC.2020.2967386

Sahoo, B. P. S., Swain, S., Wei, H. Y., and Sarkar, M., 2021. Medium Access Strategies for Integrated Access and Backhaul at mmWaves Unlicensed Spectrum, in: 2021 Wireless Telecommunications Symposium (WTS), 2021, pp. 1-6, doi: 10.1109/WTS51064.2021.9433686

Sun, S., et al., 2016. Investigation of Prediction Accuracy, Sensitivity, and Parameter Stability of Large-Scale Propagation Path Loss Models for 5G Wireless Communications, in IEEE Transactions on Vehicular Technology, 65(5), 2843-2860, May 2016, doi: 10.1109/TVT.2016.2543139

Yong, S. K.,Xia, P.,and Alberto V. G., 2011. Introduction to 60GHz, in 60GHz Technology for Gbps WLAN and WPAN: From Theory to Practice , Wiley, 2011, pp.1-16,doi: 10.1002/9780470972946.ch1

Zhang, Z., and Yu, H., 2019. Beam interference suppression in multi-cell millimeter wave communications, in Digital Communications and Networks, 5(3), 196-202, https://doi.org/10.1016/j.dcan.2018.01.003.